Simulated Changes in the Particulate Carbon Export Efficiency due to Diel Vertical Migration of Zooplankton in the North Atlantic

Thomas Gorgues[1] [ID]**, Olivier Aumont[2]** [ID]**, and Laurent Memery[3]** [ID]

[1]Univ. Brest, CNRS, IRD, Ifremer, Laboratoire d'Océanographie Physique et Spatiale (LOPS), Institut Universitaire Europeén de la Mer (IUEM), Brest, France, [2]Laboratoire d'Oceanographie et de Climatologie: Experimentation et Approches Numeriques, IPSL, Paris, France, [3]Laboratoire des Sciences de l'Environnement Marin (LEMAR), UBO/CNRS/IRD/Ifremer, Institut Universitaire Europeén de la Mer (IUEM), Plouzané, France

Abstract Diel vertical migration (DVM) of zooplankton has been recognized to influence the biological pump by releasing carbon and nutrients at depth. However, uncertainties regarding the magnitude, spatial occurrence, and variability of this "active transport," as well as its impact on the carbon export, remain. To tackle these questions, a cost-effective parameterization of the DVM is included into a regional biogeochemical model simulating the North Atlantic. In addition to a reference simulation in which no DVM is simulated, two relative biomasses of migrating zooplankton (30% and 60%) have been tested. It leads to an active to passive export ratio in agreement with published estimations and to an increase in the carbon export efficiency at 1,000 m between 20% and 40%. However, this effect is partially canceled out by a simulated primary production decrease. DVM differently impacts contrasted North Atlantic regions with the largest effect on export efficiency found in the subtropical area.

1. Introduction

Diel vertical migration (DVM) of species such as copepods and other zooplankton taxa into the twilight zone has the potential to significantly contribute to the biological pump (Buesseler et al., 2007; Kobari et al., 2008). This mechanism is driven by the predatory pressure on zooplankton, generally during daytime, that leads zooplankton to avoid visual predation by migrating from the surface into deeper layers ranging from 200- to 800-m depth according to acoustic measurements (Bianchi, Galbraith, et al., 2013). The migration depth has been shown to be related to a combination of factors such as chlorophyll, density, oxygen concentration, temperature, mixed layer depth, and incoming radiation which even includes the effect of the moonlight (Bianchi, Galbraith, et al., 2013; Bianchi, Stock, et al., 2013; Benoit-Bird et al., 2009; Hernandez-Leon et al., 2001, 2010).

During diurnal migration, a significant amount of organic matter that has been grazed in the upper ocean during nighttime is transported to this migration depth in addition to the so-called passive or gravitational flux (driven by sinking particles). This "active" transport includes both particulate and dissolved organic and inorganic carbon, released by the zooplankton species via fecal pellet production, respiration, excretion, and mortality (Buesseler & Boyd, 2009). The relative amount of the active transport of organic matter compared to the total export production (a-ratio) has been estimated to be between 15% and 40% (Bianchi, Galbraith, et al., 2013). This active transport exhibits very distinctive characteristics with regard to passive export by sinking particles. Indeed, organic and inorganic compounds are released at depth by migrating organisms and may thus escape intense remineralization in the upper mesopelagic zone. Carbon and related nutrients may therefore be very efficiently sequestered at depth by this process. DVM is thus suggested to have a strong impact on the carbon, nutrients, and oxygen distributions (Bianchi, Galbraith, et al., 2013).

DVM is therefore considered as a process that could significantly modify our understanding of the functioning of the carbon pump. Yet unresolved DVM-related questions remain as regarding its magnitude, occurrence, and its spatial and temporal variability while considering different production regimes. Indeed, DVM transport of organic matter varies regionally and temporally, depending on the biological productivity and on the zooplankton composition. Episodic measurements have shown a great variety of active transport regimes, suggesting a strong spatial variability, even if we consider the North Atlantic basin alone (Steinberg et al., 2000, 2012; Longhurst et al., 1989, 1990; Morales, 1999; Hernandez-Leon et al., 2001). However, from

AGU
100
ADVANCING EARTH
AND SPACE SCIENCE

Geophysical Research Letters

10.1029/2018GL081748

this set of sparse measurements, it is difficult to estimate accurately the contribution of DVM to export (the relative contribution of the active transport to the total export flux). Export measurements, by themselves, cannot disentangle the contribution from passive to active transport. Moreover, the dissolved components in the active transport cannot be accounted by particle measurements and sediment traps currently used in export flux observations.

Models are useful tools to analyze, quantify, and explore the role of active transport and its relative contribution to the biological pump. Previous model analyses have studied the impacts of DVM on ocean biogeochemistry either with a complex 1-D ecological model (Bianchi, Stock, et al., 2013) or with a simple 3-D ocean biogeochemical model (based on an implicit representation of the ecosystem structure with no explicit tracers for phytoplankton, zooplankton, or sinking detritus; Bianchi, Galbraith, et al., 2013). In the latter study, migrating organisms were not explicitly represented, and respiration associated to DVM was set to a uniform constant fraction of the particle production (no regional variation), that is then added to the standard remineralization of passive detritus. Finally, the interplay between ocean biogeochemistry and DVM has been recently investigated using a complex and costly end-to-end modeling setup (Aumont et al., 2018).

The main ambition of our study concerns the quantification of the active transport by DVM and its impact on the nutrients, primary production, and efficiency of the carbon export at basin scale, in the North Atlantic. We aim at analyzing changes in export ratios and at estimating the total versus active carbon export over a range of migrating zooplankton relative biomass (from 0% to 60% of total mesozooplankton biomass). To this end, as an alternative to the complex setup of Aumont et al. (2018), we have designed a simple yet cost-effective parameterization of zooplankton migration in a 3-D ocean "full" biogeochemical model (i.e., explicitly representing phytoplankton and zooplankton biomass as well as organic detritus).

2. Model Setup of the DVM

The Nucleus for European Modelling of the Ocean (Madec et al., 2008) is an ocean general circulation model used, here, in a North Atlantic regional configuration with a horizontal resolution of ¼°. It is coupled with the Pelagic Interactions Scheme for Carbon and Ecosystem Studies, which is a widely used biogeochemical model built upon the classic Nutrient-Phytoplankton-Zooplankton-Detritus architecture. Pelagic Interactions Scheme for Carbon and Ecosystem Studies simulates five nutrients (NO_3, NH_4, PO_4, Fe, and Si), two phytoplankton groups (diatoms and nanophytoplankton), two zooplankton groups (microzooplankton and mesozooplankton), and three forms (big and small sinking particles, respectively POC_b and POC_s, and dissolved) of organic matter (for a detailed model description, refer to Aumont et al., 2015).

DVM is set in the model to be performed solely by some of the mesozooplankton (i.e., 200- to 2,000-μm size class). To avoid computationally expensive explicit simulation of this mesozooplankton migration, we rather parameterized the consequences of the migration in terms of changes in organic matter fluxes. A fraction of the total mesozooplankton-related nutrients and organic matter fluxes is then transported to deeper layers and modulated according to the duration of the day. From the proportion of migrating mesozooplankton, we derived fluxes of dissolved inorganic carbon, dissolved organic carbon, big particulate carbon (POC_b), alkalinity, oxygen (O_2), phosphate (PO_4), ammonium (NH_4), and bioavailable-dissolved iron (Fe) that are released at the migration depth (detailed setup is given in Supporting Information S1). Therefore, among those elements, the organic matter experience less recycling and remineralization after being brought at the migration depth where the temperature is cooler than in the surface layers. Indeed, remineralization highly depends on temperature, with high temperatures corresponding to high remineralization rates. Using biogeochemical and physical tracers from the model, the migration depth in the model has been estimated from the formulation proposed by Bianchi, Galbraith, et al. (2013) using oxygen, temperature, surface chlorophyll, and the mixed layer depth. One distinctive feature of our setup over previously published modeling exercise (e.g., Hansen & Visser, 2016) is to allow a characterization of the effect of the DVM on nutrients concentrations and hence on the primary production.

Three numerical simulations have been run for the 1995–2005 time period, all forced by the Drakkar Forcing Set 5 fields (Dussin et al., 2014) for wind, air temperature and humidity, precipitation, and shortwave and longwave radiations. Those three simulations only differ in the parameterization of the zooplankton migration. Only the main characteristics of the simulations are given here, as a detailed description has
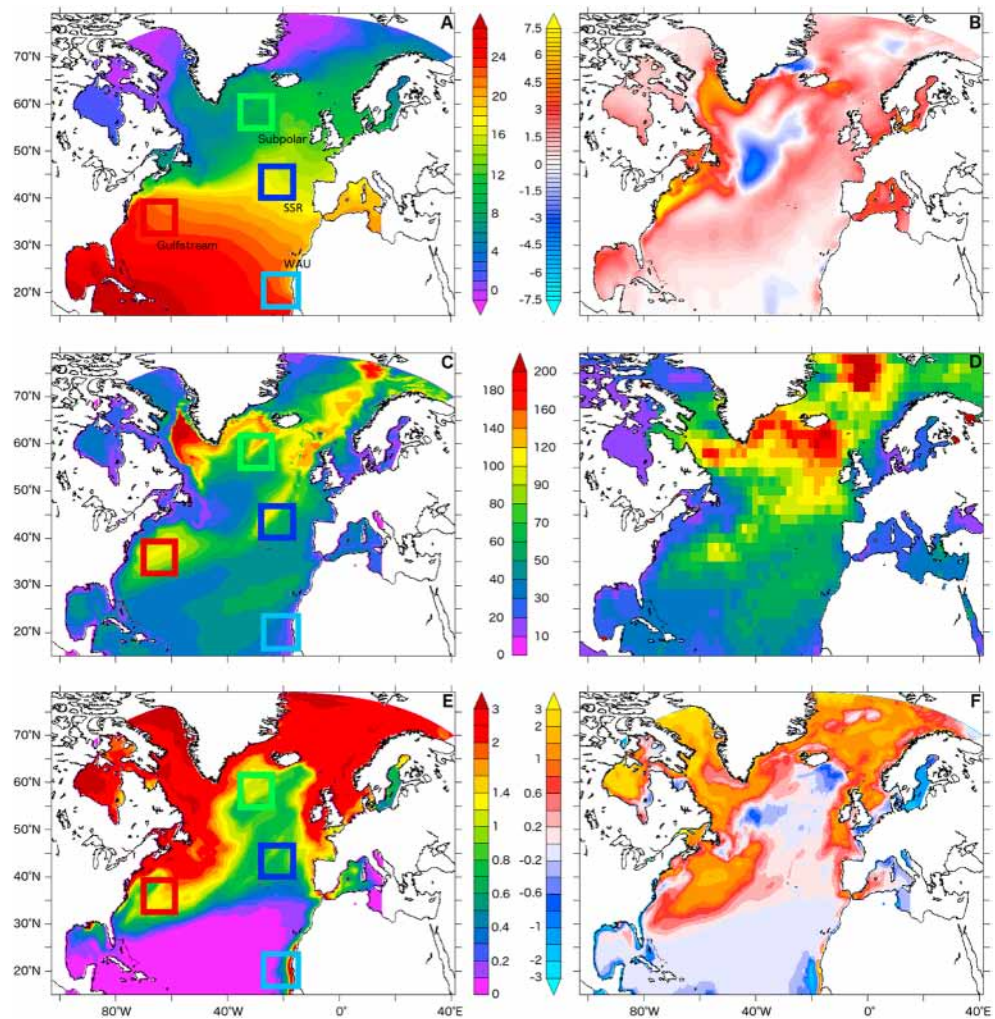
Figure 1. (a) Model Sea Surface Temperature (SST, °C) averaged between 2000 and 2005. Regions of interest are indicated: Subpolar (in green box), Subtropical Seasonally Stratified (SSR, in blue box), West African Upwelling (WAU, in light blue box), and Gulf Stream (in red box). (b) Difference between the simulated SST and the World Ocean Atlas (WOA) SST (Locarnini et al., 2006). (c) Annually averaged simulated mixed layer depth (m) over 2000 to 2005. (d) Observed Mixed layer depth (m) climatology from de Boyer Montégut et al. (2004). (e) Monthly climatological maximum surface Chlorophyll-a (mgC/m^3) over the 2000 and 2005 period in CTL. (f) Difference (mgC/m^3) between the monthly climatological simulated maximum of surface Chlorophyll and a climatology of the monthly maximum from the SeaWIFS Chlorophyll-a.

been made available as Supporting Information S1. In the first model simulation, migration of zooplankton is disabled (hereafter CTL, referring to the control run), allowing the model to perform only gravitational—or passive—particle sinking beyond the euphotic zone. In the second one, active transport is enabled (hereafter M30) with 30% of mesozooplankton considered as migrating. In the third experiment, the proportion of migrants is raised to 60% (hereafter M60). Those respective ratios correspond to the median and maximum levels of migrating versus total mesozooplankton derived from in situ data (Al-mutairi & Landry, 2001; Ariza et al., 2015; Decima et al., 2011; Steinberg et al., 2008). Testing those ratios will help in characterizing the sensitivity of ocean nutrients cycle and carbon export to active transport.

The North Atlantic basin provides a wide physical and biogeochemical diversities. This leads to different production regimes of interest for studying the spatial variability of the active transport and its consequences. Typical North Atlantic production regimes (Figure 1) encompass (i) the generally diatom-dominated spring blooms at northern latitudes (hereinafter Subpolar), (ii) the Seasonally Stratified Region (SSR), (iii) the persistently high productive regime (Gulf Stream), the West African Upwelling (WAU),
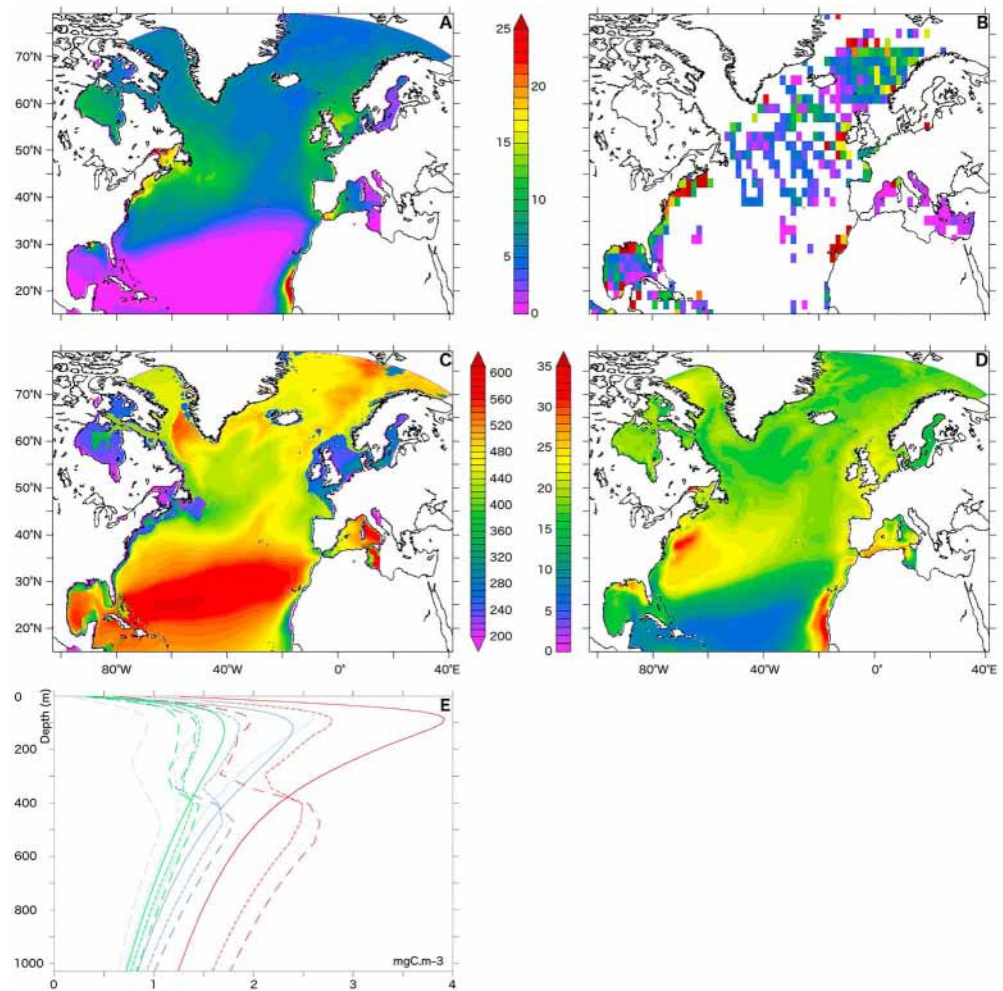
Figure 2. (a) Annually averaged concentration (mgC/m^3) of mesozooplankton in CTL over 100 m. (b) Same as (a) but with mesozooplankton concentration (mgC/m^3) from the MAREDAT database (O'Brien, 2014). (c) Migration depth (m) in M30 and M60. (d) Biomass of mesozooplankton relative to the total biomass (%) in the CTL simulation. Model outputs have been averaged over the 2000–2005 time period. (e) Big carbon particle concentration (POC_b in mgC/m^3) in the four regions (Subpolar, in green lines and dashes; SSR, in blue lines and dashes; WAU, in light blue lines and dashes; and Gulf Stream, in red lines and dashes**)** along depth during the spring bloom (April to June average) for CTL (plain lines), M30 (dashed-pointed lines), and M60 (dashed lines).

and (iv) the persistently low productive region. The latter displays, as expected, extremely weak concentrations of mesozooplankton (Figure 2a), and there is therefore virtually no possible active transport in this region for any simulated scenario. Therefore, we defined four squared areas (with a size of 12.5° by 12.5°) to characterize the Subpolar, the Subtropical, the Western African Upwelling, and the Gulfstream production regimes (Figure 1) where active transport may impact the biogeochemical cycles.

3. Results

3.1. North Atlantic Model Reference State

The Sea Surface Temperature, simulated by our model (displayed in Figure 1a), represents a realistic temperature gradient from low to high latitudes. However, some differences between the simulated Sea Surface Temperature and its data counterpart are noticeable, the most obvious being a warm bias in the Gulf Stream region and a cold bias in the North Atlantic Current region (Figure 1b) that are related to shifted locations of the Gulf Stream and the North Atlantic Current. Our simulation also displays an overestimation of the simulated Mixed Layer Depth (MLD) in the Labrador Sea (when compared to the observed MLD in

Figures 1c and 1d). Indeed, North Atlantic numerical simulations (with diverse ocean models and forcing sets) have been known to consistently display those dynamical biases if run at relatively coarse (i.e., not fully resolving mesoscale to submesoscale dynamics) resolution (see Holt et al., 2014, and references therein).

Regarding the chlorophyll (Chl) distribution in our reference simulation (CTL, Figure 1e), high productive regimes are clustered along the North American coastline and the European shelf while minima are found in the subtropical gyre, with an intermediate productive area located in the subpolar region. Compared to chlorophyll-*a* satellite-derived products, the spring bloom is more intense in CTL and hence leads to an over-estimation of simulated Chl concentration (Figures 1e and 1f) mostly noticeable north of 30°N, in places where simulated MLD are too deep (Figures 1c and 1d) in winter. However, the main large-scale patterns with low Chl concentration in the subtropical gyre as well as in the subpolar region are well captured in the model simulation (Figure 1f).

Finally, the mesozooplankton distribution (Figures 2a and 2b) simulated in CTL is close to the one derived from the observations gathered in the MAREDAT database (Buitenhuis et al., 2013; O'Brien, 2014) with maxima (located in the Gulf stream region, the Norwegian sea, and the North-East African upwelling) and minima (located in the subtropical gyre) of the same order of magnitude.

3.2. Active Transport

The migration depth in the model (Figure 2c) spans 380 to 630 m, excluding the continental shelves, where bathymetry ultimately determines the diel movement of mesozooplankton. Maximum migration depths are found in the subtropical gyre where they can exceed 600 m, while minima lie in between the subtropical and subpolar areas with depth reaching 400 m. Therefore, the overall pattern of the migration depth displays a gradient with deep migration depths in the subtropical gyre and shallower migration depth toward higher latitudes. This finding is in good agreement with results from published one-dimensional model outputs and data at sites displaying different physical and biogeochemical characteristics (Bianchi, Stock, et al., 2013).

Since in our model, the migrating biomass is set as a constant fraction of the mesozooplankton biomass, the seasonal variability of active transport follows that of mesozooplankton. In the midlatitudes and high latitudes which are characterized by a distinctive spring bloom, the maximum biomass of mesozooplankton (and hence of migrating organisms) is reached about 2 months after the peak of phytoplankton as a consequence of slower growth rates.

3.3. Active Transport Impact on Particulate Export Efficiency

In our simulations, the active transport decreases primary productivity by −12% and −20% compared to the control run in the M30 and M60 scenarios, respectively (Table 1). Consequently, the export of particulate organic carbon experiences a respective decrease by 18% and 31% at the 150-m depth horizon, in the M30 and M60 scenarios when compared to the control run. The export production at 150 m (ep_{150}-ratio, the ratio between the carbons exported at the 150-m horizon over the total primary production) is equal to 0.21 in the control run, and it decreases to 0.19 and 0.18 in the M30 and M60, respectively.

Even so the primary productivity is smaller than in the control run, the absolute amount of deep particulate export for both migration runs increases significantly. Indeed, particulate export at 1,000 m ranges, respectively, from 221 to 227 TgC/year for M30 and M60, compared to 210 TgC/year in CTL (Table 1). This represents an increase of, respectively, 5% and 8%, for M30 and M60, despite a decrease in primary productivity of −12% and −20%. This translates in an increase of the ep-ratio at 1,000 m (ep_{1000}-ratio) from 0.05 in CTL to 0.07 in M60.

The model estimate of total active transport, including particulate and dissolved organic and inorganic carbon, ranges from 166 to 281 TgC/year for the whole North Atlantic basin, that is, 25% to 50% of the gravitational flux at 150 m. This result agrees with previous estimates suggesting that active transport typically ranges around 10–50% of the sinking flux of organic particles (Bianchi, Galbraith, et al., 2013) at global scale. Aumont et al. (2018) modeling study estimated this value between 30% and 40% in midlatitudes regions, and the regional modeling study of Hansen and Visser (2016) estimated this value between 16% and 30% specifically in the North Atlantic region. The largest contribution of the active transport in the model is

Table 1
Primary Productivity (PP), Export and Active Transport (AT) for the Control, and the Migration Simulation Runs (M30 and M60) for the 2000–2005 Averaged Time Period

	Control run: CTL (0% mig)	Migration run: M30 (30% mig)	Migration run: M60 (60% mig)
PP (TgC/year)	3915	3461	3142
{change compared to Control}		−12%	−20%
Export[a] at 150 m (TgC/year)	808	665	559
{change compared to Control}		−18%	−31%
[ep_{150}-ratio]	0.21	0.19	0.18
Export[b] at 1,000 m (TgC/year)	210	221	227
{change compared to Control}		5%	8%
[ep_{1000}-ratio]	0.05	0.06	0.07
Active Transport[c] (AT; in TgC/year)		166	281
[AT/Export[a] at 150 m]		25%	50%
AT of big carbon particles (TgC/year)		98	166

Note. POC_s and POC_b are, respectively, small and big particulate organic carbon; DOC and DIC stand for Dissolved Organic and Inorganic Carbon.
[a]Defined as POC_s + POC_b (without AT).　[b]Defined as POC_s + POC_b (note that all Actively Transported carbon is put back in the water column between 380 and 630 m).　[c]Defined as POC_b + DIC + DOC.

in the form of big particulate carbon, with 98 to 166 TgC/year in M30 and M60, representing around half of the total simulated active export.

3.4. Regional Analysis of the Active Transport Effect

The four regions displayed in Figure 1 show different production regimes in the North Atlantic and may therefore present a significantly different sensitivity to the active transport. Table 2 summarizes the productivity and export variables within these four regions. Among these regions, primary productivity decreases most significantly in the WAU and then in the Gulfstream and SSR regions when compared to the Subpolar regime, where little variation (~3%) is observed independently of whether 30% or 60% of the mesozooplankton is supposed to migrate (Table 2).

Changes in export efficiency at 150 m in each regime are mirroring the local decrease in primary productivity. While exports at 150 m in the Subpolar, the SSR, and the Gulfstream regions remain almost constant, the WAU regions experience a significant decrease of almost 40%. At greater depth, the export at 1,000 m increases in the two migration scenarios for all the regions but the WAU (Table 2). However, the highest increase is found in the Gulfstream region for the M60 simulation, with a 27% increase of the export at 1,000 m (despite the decrease in primary production) when compared to the control simulation. The export efficiency at 1,000 m (ep_{1000}-ratio) increases in all four regions, if migrating zooplankton is considered, with the most significant increase (0.06 to 0.1) in the WAU region for M60.

Noticeably, the ratio of active to passive export (a-ratio) increases in all regions in both M30 and M60 with a maximum in the WAU (Table 2). Differences in the a-ratio between the M30 and M60 simulations show an increase between M30 and M60 with a slightly higher increase in the Gulfstream region.

The vertical distribution of large particulate carbon is displayed on Figure 2e. In the control run, the four regimes exhibit similar qualitative profiles, with maxima in the subsurface (between 100 and 200 m) followed by an exponential decrease deeper in the water column. As expected, the effect of the active transport is to redistribute particulate organic carbon between the subsurface and the migration depth. Therefore, the active transport of carbon decreases the concentration of particles in the subsurface while increasing it deeper than ~500 m. Those characteristic profiles have noticeably been observed in equatorial regions by Kiko et al. (2017). Interestingly, in M60, the amount of big particles can even be higher at the migration depth, than in the subsurface layer. The WAU is the only region where the added POC_b at depth (in M30 and M60) is not sufficient to exceed the POC_b concentration of CTL. It also has to be noted that the WAU region shows the largest dispersion between the two scenarios.

4. Discussion

The first unequivocal effect of the vertical migration by zooplankton evidenced by our model experiments is the direct removal of nutrients and organic matter from the surface through active transport, which in turn

Table 2

Primary Productivity (PP), Export, and Active transport (AT) for the Different Regions in the Migration Simulation Runs, Showing Control (CTL), 30% (M30), and 60% (M60) for the 2000–2005 Averaged Time Period

	Subpolar			SSR			Gulf Stream			WAU		
	CTL	M30	M60	CTL	M30	M60	CTL	M30	M60	CTL	M30	M60
PP (mgC·m⁻²·day⁻¹)	240	−5	−8	423	−45	−82	596	−67	−118	691	−241	−332
Export at 150 m (mgC·m⁻²·day⁻¹)	70	=	=	92	−7	−13	121	−2	−8	143	−53	−56
ep_{150}-ratio	0.29	=	=	0.22	=	=	0.20	+0.02	+0.03	0.21	−0.01	+0.03
Export at 1,000 m (mgC·m⁻²·day⁻¹)	25	+1	+2	30	+1	+1	33	+6	+9	46	−6	−9
ep_{1000}-ratio	0.1	+0.01	+0.02	0.07	+0.01	+0.02	0.06	+0.01	+0.03	0.06	+0.02	+0.04
Active Transport (mgC·m⁻²·day⁻¹)		+12	+23		+18	+31		+35	+57		+35	+50
a-ratio		+0.17	+0.32		+0.2	+0.39		+0.29	+0.50		+0.38	+0.57
Particulate active transport mgC.m⁻².day⁻¹		+7	+14		+11	+19		+21	+34		+22	+30

Note. Results for M30 and M60 are given relatively to CTL (i.e., numbers are differences between M30 and CTL and M60 and CTL).

has a direct negative impact on the primary production of the whole North Atlantic (Table 1). Indeed, DVM transports organic material deeper in the water column than the passive export (characteristic profiles of POC_b in Figure 2e), which decreases the vertical input of nutrients into the surface productive layer.

This prominent decrease in primary productivity induces an expected decrease in the carbon export by sinking particles at 150 m. However, it does not induce the expected decrease in carbon export to the deep ocean (at 1,000 m). On the contrary, we note, in M30 and M60, an increase in the absolute export at 1,000 m, which is explained by the active transport of organic particles escaping remineralization from the surface to the migration depth (Table 1). Moreover, remineralization of particles is known to be higher in warm waters than in cold waters (Marsay et al., 2015, and references therein). Therefore, carbon particles transported from the surface to the migration depth have overall been less remineralized, thus explaining the increase in the export efficiency at 1,000 m (Table 1). Such an increase in the export efficiency applied to satellite-derived primary production would result in a revised carbon export estimation. As an example, an increased efficiency of the carbon export of 0.01 (to be compared with our values of the ep_{1000}-ratio in Table 1) at global scale would result in a 0.5 Gt C/year increase of the carbon export toward the ocean interior (based on a PP of 50 Gt C/year, Carr et al., 2006; and our ep_{1000}-ratio).

Given our modeling setup, the M60 scenario presented in this study has been designed to be an upper bound of the zooplankton DVM impacts in the North Atlantic. Indeed, we consider in our modeling setup that mesozooplankton produces fecal pellets during its stay in its deep habitat. This parameterization is justified by the high uncertainty related to the gut clearance time of the mesozooplankton from few tens of minutes to few hours (Baars & Oosterhuis, 1984; Dagg & Walser, 1987; Mackas & Bohrer, 1976; Morales et al., 1990) that has to be compared to the vertical migration duration of the order of 1 hr (Wiebe et al., 1992). As an example, Atkinson et al. (1996) estimated that, near South Georgia, 61% to 77% of ingested material in the surface remain in mesozooplankton guts during the migration. Obviously, our assumption maximizes the production of particulate organic carbon by migrating organisms in the mesopelagic domain. Moreover, the mesozooplankton fluxes imposed at the migration depth are computed using the temperature within the "surface" layers, where lies the simulated biomass of mesozooplankton. As a result, our simulations neglect the impact that a lower temperature (found at the migration depth) could have on the mesozooplankton physiological rates. This simplifying hypothesis will again lead to an overestimation of mesozooplankton respiration fluxes and organic matter production rates at the migration depth. Finally, in agreement with station data (Al-mutairi & Landry, 2001; Decima et al., 2011; Steinberg et al., 2008), the ratio of migrants versus total zooplankton has been found to regionally vary between 0% and 60%. The modeling study of Aumont et al. (2018) does display a weaker spatial variability (between 25% and 45%) of this ratio in the North Atlantic, while, in our setup, a constant ratio is applied over the whole domain.

Despite the latter approximation, the impacts of DVM display regional differences in our simulations. Indeed, the decrease in primary production is less pronounced in the Subpolar region (3% decrease in M60) where the deep MLD allows nutrients released at the migration depth to eventually come back in the euphotic zone (Table 2). In the SSR as well as in the Gulfstream regions, primary production decreases more significantly by ~20% in the M60 scenario, while the maximum decrease is reached in the WAU (~50% in M60). However, the increase in the export to the deep ocean is maximum in the Gulfstream region with an increase by almost 30% of the carbon export compared to less than 10% in the SSR and Subpolar regions and even a slight decrease in the WAU (Table 2 and Figure 2e). However, this latter decrease does not reflect the WAU increase in carbon export efficiency (ep_{1000}-ratio) but is rather the result of the decrease in primary production for M30 and M60. This result suggests that active transport is influenced by the food web structure. A year-round high ratio of zooplankton (see Figure 2d), as in the WAU, makes the active transport highly effective but also highly sensitive to a modification of the primary production. Less stable ecosystem that favors seasonal large

phytoplankton ecosystem composition already allows high efficiency of carbon export in deep ocean (e.g., see ep_{1000}-ratio and a-ratio for the Subpolar region) and is less impacted by active transport. Therefore, the WAU and the Gulfstream regions appear as the regions that are the most sensitive to the vertical migration of zooplankton with a respective decrease in primary production of ~50% and ~20% in M60. The most significant increase in carbon export to the deep ocean (~30% in M60) is observed for the Gulfstream region even if the higher a-ratios are attributed to the WAU for both scenarios (Table 2). Those regional specificities are consistent with the regional structuration of the ecosystem with the highest simulated ratio of mesozooplankton over the total biomass (Figure 2d). More generally, the relative contribution of the active transport suggests a maximum effect in productive regions (with relatively high concentration of mesozooplankton), increasing their effectiveness at exporting carbon to the ocean interior.

5. Conclusions

Our study advocates that active transport by migrating zooplankton is a contribution to the biological pump relevant enough to be included in contemporary biogeochemical models for present and future climate projections. Indeed, even assuming that only 30% of epipelagic mesozooplankton migrates, a decrease in primary production of 12% due to a deeper export of organic material has been stressed. Moreover, an increase of 5% of the carbon export at 1,000 m has been estimated despite this concomitant decrease of the primary production.

This realistic simulation of the biogeochemical state of the North Atlantic (i.e., using interannual realistic forcing), which takes into account some aspects of the zooplankton migration, shows a significant spatial variability regarding the impact of active transport. The ecosystem structure is the primary driver of this spatial variability. Highly productive regions that can sustain elevated concentrations of mesozooplankton, like the WAU and Gulfstream regions, show a remarkable response to DVM, leading to significant changes in the vertical profiles of large particles (with characteristic maxima at two depths) and ultimately the carbon export by those particles.

Large uncertainties remain in model estimates, linked in particular to the representation and parameterization of the zooplankton metabolism or the gut digestion times. Moreover, our model is not representing organisms larger than 2 mm, while ADCP data showed DVM of zooplankton and micronekton ranging from millimeter to centimeter scale (Bianchi, Galbraith, et al., 2013). The micronekton DVM, which could accentuate the overall DVM impacts, is therefore not taken into account in our model. But despite those approximations, our simulations are able to capture the first-order impacts of migrating zooplankton on carbon export with active versus passive transport ratios in agreement with those from the 1-D explicit model of Bianchi, Stock, et al. (2013) or 3-D models (Aumont et al., 2018). Yet cost-effective accurate parameterizations are needed to include this process into global biogeochemical model configurations and particularly in the Intergovernmental Panel on Climate Change (IPCC) class models for future carbon budget model estimates.

References

Al-mutairi, H., & Landry, M. R. (2001). Active export of carbon and nitrogen by diel migrant zooplankton at station ALOHA. *Deep-Sea Research Part II*, *48*(8-9), 2083–2103. https://doi.org/10.1016/S0967-0645(00)00174-0

Ariza, A., Garijo, J. C., Landeira, J. M., Bordes, F., & Hernandez-Leon, S. (2015). Migrant biomass and respiratory carbon flux by zooplankton and micronekton in the subtropical northeast Atlantic Ocean (Canary Islands). *Progress in Oceanography*, *134*, 330–342. https://doi.org/10.1016/j.pocean.2015.03.003

Atkinson, A., Ward, P., & Murphy, E. J. (1996). Diel periodicity of subantarctic copepods: Relationships between vertical migration, gut fullness and gut evacuation rate. *Journal of Plankton Research*, *18*(8), 1387–1405. https://doi.org/10.1093/plankt/18.8.1387

Aumont, O., Ethé, C., Tagliabue, A., Bopp, L., & Gehlen, M. (2015). PISCES-v2: An ocean biogeochemical model for carbon and ecosystem studies. *Geoscientific Model Development*, *8*(8), 2465–2513. https://doi.org/10.5194/gmd-8-2465-2015

Aumont, O., Maury, O., Lefort, S., & Bopp, L. (2018). Evaluating the potential impacts of the diurnal vertical migration by marine organisms on marine biogeochemistry. *Global Biogeochemical Cycles*, *32*(11), 1622–1643. https://doi.org/10.1029/2018GB005886

Baars, M. A., & Oosterhuis, S. S. (1984). Diurnal feeding rhythms in North Sea copepods measured by gut fluorescence, digestive enzyme activity and grazing on labelled food. *Netherlands Journal of Sea Research*, *18*(1-2), 97–119. https://doi.org/10.1016/0077-7579(84)90027-9

Benoit-Bird, K. J., Au, W. W. L., & Wisdom, D. W. (2009). Nocturnal light and lunar cycle effects on diel migration of micronekton. *Limnology and Oceanography*, *54*(5), 1789–1800. https://doi.org/10.4319/lo.2009.54.5.1789

Bianchi, D., Galbraith, E. D., Carozza, D. A., Mislan, K. A. S., & Stock, C. A. (2013). Intensification of open-ocean oxygen depletion by vertically migrating animals. *Nature Geoscience*, *6*(7), 545–548. https://doi.org/10.1038/ngeo1837

Bianchi, D., Stock, C., Galbraith, E. D., & Sarmiento, J. L. (2013). Diel vertical migration: Ecological controls and impacts on the biological pump in a one-dimensional ocean model. *Global Biogeochemical Cycles*, *27*, 478–491. https://doi.org/10.1002/gbc.20031

Buesseler, K. O., & Boyd, P. W. (2009). Shedding light on processes that control particle export and flux attenuation in the twilight zone of the open ocean. *Limnology and Oceanography*, *54*(4), 1210–1232. https://doi.org/10.4319/lo.2009.54.4.1210

Buesseler, K. O., Lamborg, C. H., Boyd, P. W., Lam, P. J., Trull, T. W., Bidigare, R. R., et al. (2007). Revisiting carbon flux through the ocean's twilight zone. *Science*, *316*(5824), 567–570. https://doi.org/10.1126/science.1137959

Buitenhuis, E. T., Vogt, M., Moriarty, R., Bednarsek, N., Doney, S. C., Leblanc, K., et al. (2013). MAREDAT: Towards a world atlas of MARineEcosystem DATa. *Earth System Science Data*, *5*(2), 227–239.

Carr, M.-E., Friedrichs, M. A. M., Schmeltz, M., Aita, M. N., Antoine, D., Arrigo, K. R., et al. (2006). A comparison of global estimates of marine primary production from ocean color. *Deep-Sea Research Part II*, *53*(5-7), 741–770. https://doi.org/10.1016/j.dsr2.2006.01.028

Dagg, M. J., & Walser, W. E. (1987). Ingestion, gut passage, and egestion by the copepod Neocalanus plumchrus in the laboratory and in the subarctic Pacific Ocean. *Limnology and Oceanography*, *32*(1), 178–188. https://doi.org/10.4319/lo.1987.32.1.0178

de Boyer Montégut, C., Madec, G., Fischer, A. S., Lazar, A., & Iudicone, D. (2004). Mixed layer depth over the global ocean: An examination of profile data and a profile-based climatology. *Journal of Geophysical Research*, *109*, C12003. https://doi.org/10.1029/2004JC002378

Decima, M., Landry, M. R., & Rykaczewski, R. (2011). Broad-scale patterns in mesozooplankton biomass and grazing in the eastern equatorial Pacific. *Deep-Sea Research Part II*, *58*(3-4), 387–399. https://doi.org/10.1016/j.dsr2.2010.08.006

Dussin, R., Barnier, B., & Brodeau, L. (2014). The making of Drakkar forcing set DFS5. DRAKKAR/MyOcean Report 05-10-14,.

Hansen, A. N., & Visser, A. W. (2016). Carbon export by vertically migrating zooplankton: an optimal behavior model. *Limnology and Oceanography*, *61*(2), 701–710. https://doi.org/10.1002/lno.10249

Hernandez-Leon, S., Almeida, C., Yebra, L., Aristegui, J., De Puelles, M. L. F., & Garciia-Braun, J. (2001). Zooplankton abundance in subtropical waters: Is there a lunar cycle? *Scientia Marina*, *65*(S1), 59–64. https://doi.org/10.3989/scimar.2001.65s159

Hernandez-Leon, S., Franchy, G., Moyano, M., Menendez, I., Schmoker, C., & Putzeys, S. (2010). Carbon sequestration and zooplankton lunar cycles: Could we be missing a major component of the biological pump? *Limnology and Oceanography*, *55*(6), 2503–2512. https://doi.org/10.4319/lo.2010.55.6.2503

Holt, J., Allen, J. I., Anderson, T. R., Brewin, R., Butenschön, M., Harle, J., et al. (2014). Challenges in integrative approaches to modelling the marine ecosystems of the North Atlantic: Physics to fish and coasts to ocean, Prog. *Oceanography*, *129*, 285–313. https://doi.org/10.1016/j.pocean.2014.04.024

Kiko, R., Biastoch, A., Brandt, P., Cravatte, S., Hauss, H., Hummels, R., et al. (2017). Biological and physical influences on marine snowfall at the equator. *Nature Geoscience*, *10*(11), 852–858. https://doi.org/10.1038/NGEO3042

Kobari, T., Steinberg, D. K., Ueda, A., Tsuda, A., Silver, M. W., & Kitamura, M. (2008). Impacts of ontogenetically migrating copepods on downward carbon flux in the western subarctic Pacific Ocean. *Deep-Sea Research Part Ii-Topical Studies in Oceanography*, *55*(14-15), 1648–1660. https://doi.org/10.1016/j.dsr2.2008.04.016

Locarnini, R, A, Mishonov, A. V., Antonov, J. I., Boyer, T. P., & Garcia, H. E. (2006). World Ocean Atlas 2005, Volume 1: Temperature. In S. Levitus (Ed.), *NOAA Atlas NESDIS* (Vol. 61, 182 pp.). Silver Spring, MD: NOAA.

Longhurst, A. R., Bedo, A., Harrison, W. G., Head, E. J. H., Horne, E. P., Irwin, B., & Morales, C. (1989). NFLUX: A test of vertical nitrogen fluxby diel migrant biota. *Deep Sea Research Part A. Oceanographic Research Papers*, *36*(11), 1705–1719. https://doi.org//10.1016/0198-0149(89)90067-8

Longhurst, A. R., Bedo, A. W., Harrison, W. G., Head, E. J. H., & Sameoto, D. D. (1990). Vertical flux of respiratory carbon by oceanic diel migrant biota. *Deep-Sea Research*, *37*(4), 685–694.

Madec, G., & the NEMO team (2008). NEMO ocean engine. Note du Pole de modélisation, Institut Pierre-Simon Laplace (IPSL). (No. 27). France.

Mackas, D. L., & Bohrer, R. (1976). Fluorescence analysis of zooplankton gut contents and an investigation of diel feeding patterns. *Journal of Experimental Marine Biology and Ecology*, *25*(1), 77–85. https://doi.org/10.1016/0022-0981(76)90077-0

Marsay, C. M., Sanders, R. J., Henson, S. A., Pabortsava, K., Achterberg, E. P., & Lampitt, R. S. (2015). Attenuation of sinking particulate organic carbon flux through the mesopelagic ocean. *PNAS*, *112*(4), 1089–1094. https://doi.org/10.1073/pnas.1415311112

Morales, C. E. (1999). Carbon and nitrogen fluxes in the oceans: the contribution by zooplanktonmigrants to active transport in the North Atlantic during the Joint Global Ocean Flux Study. *Journal of Plankton Research*, *21*, 1799–1808.

Morales, C. E., Bautista, B., & Harris, R. P. (1990). Estimates of ingestion in copepod assemblages: gut fluorescence in relation to body size. In M. Barnes & R. N. Gibson (Eds.), *Trophic relationships in the marine environment* (pp. 565–577). Aberdeen: Aberdeen University Press.

O'Brien, T. D. (2014). COPEPOD: The Global Plankton Database. An overview of the 2014 database contents, processing methods, and access interface. U.S. Dep. Commerce, NOAA Tech. Memo., NMFS-F/ST-37 (29 pp.).

Steinberg, D. K., Carlson, C. A., Bates, N. R., Goldthwait, S. A., Madin, L. P., & Michaels, A. F. (2000). Zooplankton vertical migration and the active transport of dissolved organic and inorganic carbon in the Sargasso Sea. *Deep-Sea Research Part I-Oceanographic Research Papers*, *47*(1), 137–158. https://doi.org/10.1016/s0967-0637(99)00052-7

Steinberg, D. K., Cope, J. S., Wilson, S. E., & Kobari, T. (2008). A comparison of mesopelagic zooplankton community structure in the subtropical and subarctic Pacific Ocean. *Deep-Sea Research Part II*, *55*, 1594–1604.

Steinberg, D. K., Lomas, M. W., & Cope, J. S. (2012). Long-term increase in mesozooplankton biomass in the Sargasso Sea: Linkage to climateand implications for food web dynamics and biogeochemical cycling. *Global Biogeochemical Cycles*, *26*, GB1004. https://doi.org/10.1029/2010GB004026

Wiebe, P. H., Copley, N. J., & Boyd, S. H. (1992). Coarse-scale horizontal patchiness and vertical migration of zooplankton in Gulf Stream warm-core ring 82-H. *Deep-Sea Research*, *39*, S247–S278.